AGU PUBLICATIONS

Geophysical Research Letters

RESEARCH LETTER
10.1002/2014GL059471

Key Points:
- Significant changes in chemical weathering and associated phosphorus release have occurred since 1850
- The strength of the weathering feedback is of second order

Supporting Information:
- Readme
- Text S1

Correspondence to:
D. S. Goll,
daniel.goll@mpimet.mpg.de

Citation:
Goll, D. S., N. Moosdorf, J. Hartmann, and V. Brovkin (2014), Climate-driven changes in chemical weathering and associated phosphorus release since 1850: Implications for the land carbon balance, *Geophys. Res. Lett.*, *41*, 3553–3558, doi:10.1002/2014GL059471.

Received 22 FEB 2014
Accepted 1 MAY 2014
Accepted article online 6 MAY 2014
Published online 22 MAY 2014

Climate-driven changes in chemical weathering and associated phosphorus release since 1850: Implications for the land carbon balance

Daniel S. Goll[1], Nils Moosdorf[2], Jens Hartmann[2], and Victor Brovkin[1]

[1]Land in the Earth System, Max Planck Institute for Meteorology, Hamburg, Germany, [2]Institute for Geology, Center for Earth System Research and Sustainability, University of Hamburg, Hamburg, Germany

Abstract Chemical weathering and associated nutrient release act as a control on atmospheric carbon dioxide (CO_2) concentration. To globally quantify the contribution of chemical weathering and associated phosphorus (P) release on the historical trend in terrestrial carbon uptake, we applied a weathering model under climate reconstructions from four Earth System Models. In these simulations, CO_2 consumption and P release increased from 1850 to 2005 by 11 ± 3% and 12 ± 4%, respectively. Thereby the intensification of weathering due to climate change could have contributed to a small extent to the trend in terrestrial carbon uptake since the pre–Industrial Period. Using a back of the envelope calculation, we found a feedback strength of CO_2 consumption and P release of -0.02 ± 0.01 W m^{-2} K^{-1} and -0.02 ± 0.01 W m^{-2} K^{-1}, respectively. Although being one magnitude smaller than the carbon cycle feedback, the weathering feedbacks are comparable in strength to small second-order feedbacks such as methane, fire, or ozone.

1. Introduction

Since the start of the pre–Industrial Revolution, the atmospheric carbon dioxide (CO_2) concentration has increased from 280 ppmv in 1850 up to 394 ppmv (2012), a level unprecedented in the last 2 million years [*Hoenisch et al.*, 2009].

The atmospheric CO_2 concentration is intimately linked to global climate: increased CO_2 causes a rise in surface temperature, precipitation, and runoff. All these climatic changes impact the chemical weathering of rocks, which in turn acts as a control on atmospheric CO_2 concentration on geological time scale [*Walker et al.*, 1981; *Berner et al.*, 1983].

Various studies have quantified the present-day flux of CO_2 consumption by chemical weathering. Estimates range between 0.11 and 0.44 Gt C yr^{-1} [see *Hartmann et al.* 2009, and references therein]. It was shown that current climatic changes have an effect on weathering rates. Using data from Iceland river catchments, *Gislason et al.* [2009] showed that warming correlates with an increase in chemical weathering fluxes, which corresponds to an increase in chemical weathering rate of 4–14% for each degree of temperature rise. Using a process-based model, *Beaulieu et al.* [2010, 2012] showed for the Mackenzie catchment that CO_2 consumption increases between 2.4 and 28% per 100 ppmv increase in CO_2.

The effect of climate change on weathering depends strongly on local lithological and climatic conditions [*Gislason et al.*, 2009; *Beaulieu et al.*, 2010, 2012]. Therefore, the upscaling from studies on catchment scale to global scale is problematic but can serve as a first approximation. Extrapolating model simulations for the Mackenzie catchment, *Beaulieu et al.* [2012] suggest that changes in CO_2 consumption could explain about 40% of the trend in global land C uptake since 1750. Such a high contribution of chemical weathering to the historical land C balance would imply a need for revision of our current understanding of the historical changes in the C cycle, as changes in weathering are considered negligible on this time scale. As a global study accounting for the spatial heterogeneity in lithology and climate change is missing, the global significance of changes in CO_2 consumption are still elusive.

In addition to the CO_2 consumption by chemical weathering, changes in weathering affect biological CO_2 fixation via the release of nutrients. Nutrient availability is a key regulator of the carbon balance of ecosystems, globally [*Fernandez-Martinez et al.*, 2014]. In particular, phosphorus (P) limits biological CO_2 fixation in terrestrial, freshwater, and marine systems [*Elser et al.*, 2007]. Rising CO_2 concentrations and increasing

nitrogen availability from various human-induced inputs to natural ecosystems are likely to further exacerbate P limitation, as these increases are not paralleled by a similar increase in phosphorus inputs [*Goll et al.*, 2012; *Peñuelas et al.*, 2013]. Despite an overuse of P fertilizer in developed countries, insufficient amounts are applied in developing countries [*van der Velde et al.*, 2013]. Thus, the majority of terrestrial ecosystems rely on the release of P from minerals as their primary P input. It has been recognized that climate-driven changes in P release constrain biological CO_2 fixation on geological time scales, but this aspect is usually overlooked in C cycle studies focusing on shorter time scales.

To quantify the effect of recent climatic changes on weathering related changes in CO_2 consumption and biological CO_2 fixation, we applied a weathering model under reconstructions of historical climate change from four Earth System Models (ESM).

2. Methods

We applied a spatial explicit model of chemical weathering and associated release of P which was calibrated on 381 catchments in Japan [*Hartmann et al.*, 2009]. It describes chemical weathering as function of runoff and lithology and is corrected for temperature and soil shielding effects [*Hartmann et al.*, 2014]. The temperature dependence is represented by an Arrhenius function based on apparent activation energies of different rock types, whereas the soil shielding effect depends on the soil type. P release is calculated as function of chemical weathering rates and P content in the weathering rock [*Hartmann and Moosdorf*, 2011]. Input data of the weathering model calibration are runoff [*Fekete*, 2002], lithology [*Hartmann and Moosdorf*, 2012], 2 m air temperature [*Hijmans et al.*, 2005], and soil types [*FAO et al.*, 2009].

We applied the weathering model with different climatic forcings. To quantify the effect of historic climate change on weathering rates, we derived runoff and 2 m air temperature from simulations of four different ESM (see supporting information). These simulations were performed for the Coupled Model Intercomparison Project Phase 5 (CMIP5) [*Taylor et al.*, 2012] and aim at reconstructing climate from 1850 to 2005 under the influence of natural and anthropogenic forcings derived from observations. We selected a subset of the models used in the CMIP5 project which is representative for the spread in simulated climate for present-day and past changes of all models [*Anav et al.*, 2013]. The climatic forcings from the ESM were then used to derive time series of CO_2 consumption and P release using the weathering model (STD). Additionally, we derived present-day fluxes of consumption and release using observed runoff and temperature (OBS). To analyze the effect of temperature on weathering rates, we performed additional simulations in which we either held temperature fixed on the pre-Industrial level throughout the whole time period (Tfix) or modified the apparent activation energy (E_a) in the Arrhenius term used in the weathering model (lowEa, highEa) by $\pm$ 20 kJ/mol. This range is about as twice as large as the range of E_a identified from a compilation of catchment studies [*Hartmann et al.*, 2014]. We use a wider range as the field data are rather restricted and laboratory experiments indicate an average range of E_a between 50 and 80 kJ/mol [*White et al.*, 1999]. To analyze the effect of biases in simulated runoff, we performed simulations forced by temperature simulated by ESM but observation based runoff from *Fekete* [2002] (RUN). All input fields of the weathering model were regridded prior use to a Gaussian T63 grid. We account for subgrid heterogeneity in lithology by averaging the weathering parameters for each T63 grid cell on high resolution (1 km $\times$ 1 km).

3. Results and Discussion

3.1. Present-Day Evaluation

The ability of the four selected ESM to simulate historical climate variability is discussed in detail in other publications [*Anav et al.*, 2013; *Brands et al.*, 2013]. Here we focus on the deviations in simulated runoff and temperature from observations. The average mean surface temperatures over land (excluding the Antarctica) for present day of all models is 13.3 $\pm$ 0.7°C (standard deviation) (Figure 1e), whereas the mean temperature from observational data is 13.4°C [*Anav et al.*, 2013]. Overall, the performances of the models to simulate present-day (1986–2005) temperature at a single grid cell are good as the root-mean-square errors (RMSEs) between observed and simulated temperatures that lie between 2.0 and 3.2°C (supporting information).

Present-day runoff rates are reproduced less realistically by the ESM than temperature (supporting information), as runoff is the product of several processes (e.g., precipitation, evapotranspiration, condensation, and transport) which are challenging to simulate in an ESM framework [*Randall et al.*, 2007]. The simulated

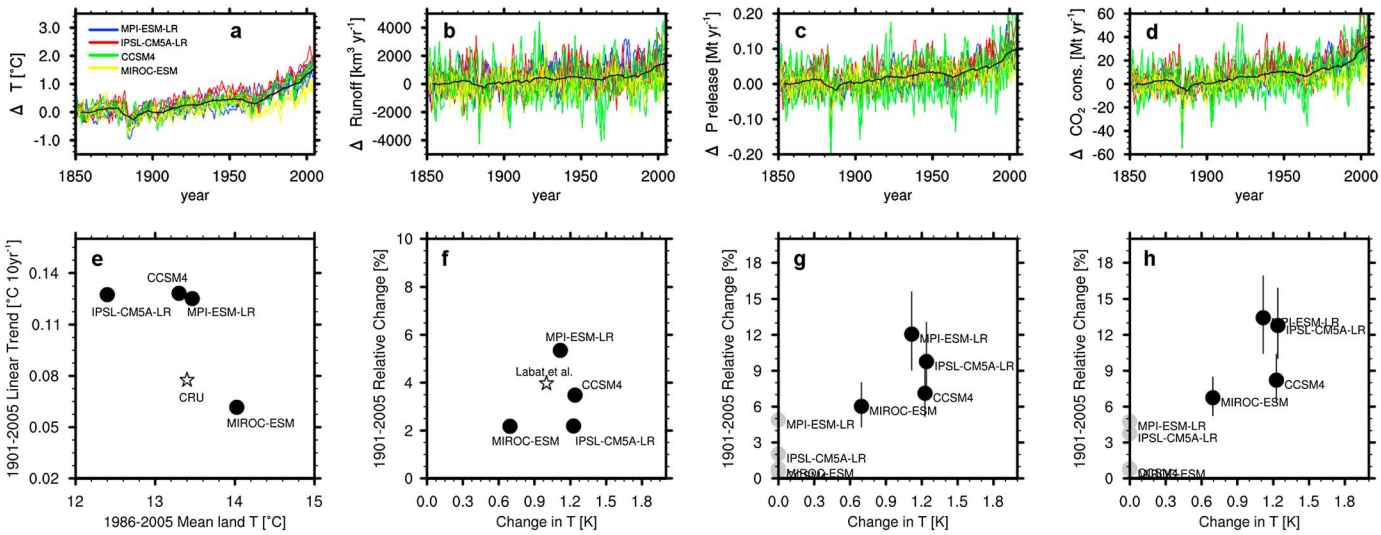

Figure 1. Globally averaged 2 m air temperature (a) over land (excluding Antarctica), (b) global runoff as simulated by the ESM, (c) relative changes in global P release, and (d) CO_2 consumption as simulated by the weathering model using the average flux from 1850 to 1879 as baseline. Each color line indicates a single simulation, the multimodel 10 year running means is shown in black. Intercomparison of (e) air temperature, (f) runoff, (g) P release, and (h) CO_2 consumption as simulated (dots) with reference to observation based estimates (stars) if available. Scatterplot in Figure 1e shows on the *x* axis the mean global temperature for present day, and on the *y* axis the linear trends over the period 1901–2005. The temperature observations are from *Anav et al.* [2013] based on Climatic Research Unit reanalysis data. The runoff observation is from *Dai and Trenberth* [2002]. Scatterplots in Figures 1f–1h show on the *x* axis the change in global temperature from 1901 to 2005, and on the *y* axis the relative change in global fluxes. The observation based sensitivity of runoff to temperature is from *Labat et al.* [2004]. Vertical lines indicate the range of uncertainty, which is based on the simulations with the modified apparent activation energy of weathering. The grey dots show the simulated fluxes when temperature is kept constant on preindustrial level throughout the whole time period.

global fluxes lie between 23,000 and 42,500 $km^3\ yr^{-1}$. Using a compilation of river discharge measurements *Fekete* [2002] estimated global runoff to be 38, 300 $km^3\ yr^{-1}$. *Dai and Trenberth* [2002] estimated a comparable flux of $37,288 \pm 662\ km^3\ yr^{-1}$ using station data and a river transport model. The root-mean-square errors (RMSEs) between simulated and the observation based runoff by *Fekete* [2002] range from 405 to 497 mm a^{-1}, which is about 100 mm a^{-1} higher than global-averaged runoff. Although 50% of the land area runoff is monitored with most measurements having an accuracy in the order of 10–20% [*Fekete*, 2002], regional fluxes, in particular at low latitudes [*Moquet et al.*, 2011], are prone to much higher uncertainty [*Dai and Trenberth*, 2002]. Nonetheless, most of the differences can be attributed to model deficits in simulating either precipitation or evapotranspiration or to the missing representation of human water management, which was shown to affect runoff regionally [*Dai and Trenberth*, 2002].

When the weathering model is forced with temperature and runoff from observations (OBS), the global CO_2 consumption and P release is 227 Mt C yr^{-1} and 1.2 Mt P yr^{-1}, respectively. The use of a rather low resolution compared to previous studies using the same weathering model [*Hartmann et al.*, 2009; *Hartmann and Moosdorf*, 2011; *Hartmann et al.*, 2014] has a very minor effect on global P release and CO_2 consumption (supporting information). When the weathering model is forced with temperature and runoff from the ESM (STD), the simulated global P release and global CO_2 consumption range between 0.8 and 1.2 Mt P yr^{-1} and 214–334 Mt C yr^{-1}, respectively (Figure 1). In case of CO_2 consumption, the simulated fluxes lie in the range of earlier estimates [*Hartmann et al.*, 2009]. For P release the simulated fluxes are comparable to earlier estimates ranging from 1.2 to 1.9 Mt P yr^{-1} [*Wang et al.*, 2010; *Hartmann et al.*, 2014]. It must be noted that the existing high estimate of 1.9 Mt P yr^{-1} is derived from upscaling a few point measurements from literature [*Wang et al.*, 2010] and therefore must be considered highly uncertain.

The RMSEs of CO_2 consumption and P release calculated from ESM derived runoff and temperature (using the observation driven model results as reference) lie between 3.6–6.4 t C $km^{-2}\ yr^{-1}$ and 16.4–23.1 kg P $km^{-2}\ yr^{-1}$, respectively. The simulated present-day fluxes are strongly affected by the biases in the runoff derived from the ESM. This is illustrated by a reduction of the RMSE of CO_2 consumption by 17–53% and the RSME of P release by 77–88% in simulations in which ESM temperature and observed runoff was used (RUN).

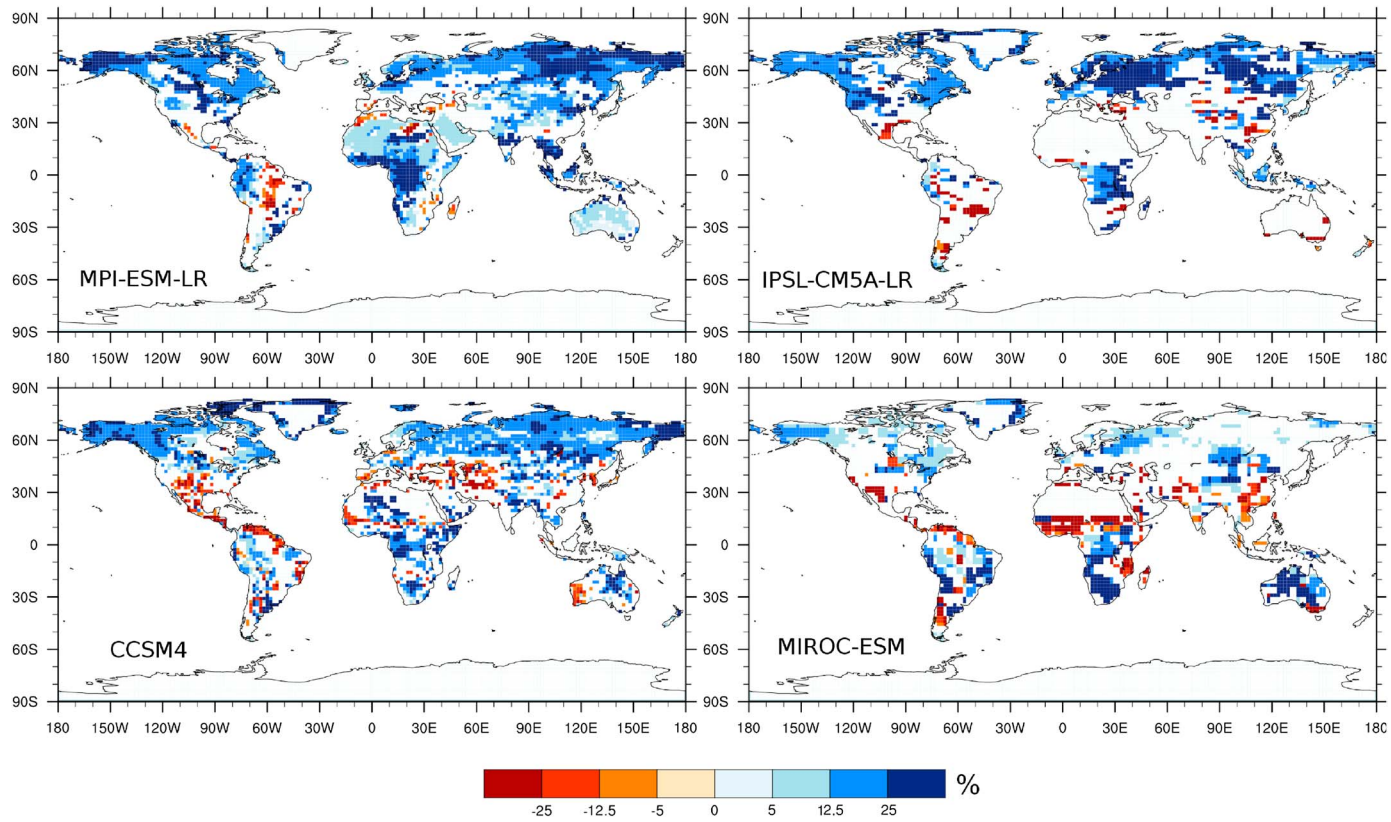

Figure 2. Change in weathering rates since 1850 according to climate reconstructions from four ESM. Shown are the ensemble means of the relative difference (%) in chemical weathering rates between the period 1986–2005 and 1850–1879. White areas mark points where either the average runoff during the reference period is zero or the difference in weathering between the two periods is statistically insignificant (*t* test; confidence level 95%).

3.2. Changes Since 1850

All ESM simulate an increase in global temperature and runoff (Figures 1a and 1b). The climatic trends are estimated by the linear trend value obtained from a least squares fit line computed for the period 1901–2005. The trend in global mean temperature is 0.08 K/decade in the observations [*Anav et al.*, 2013], and the multimodel average trend is with 0.11 $\pm$ 0.03 K decade^{-1} somewhat higher (Figure 1e). A more detailed discussion on changes in temperature in historical simulations of the CMIP5 project can be found in *Anav et al.* [2013]. An analysis of the trends in runoff from major rivers from 1920 to 1996 suggest an increase in global runoff of 4% for each degree of temperature increase [*Labat et al.*, 2004], confirming an earlier study by *Probst and Tardy* [1987]. The ESM simulate on average a comparable increase in global runoff of 3.0 $\pm$ 1.1% per 1°C increase in temperature (Figure 1f). This indicates that ESM, although having difficulties in simulating the present-day state of runoff, are able to simulate changes in runoff consistent with changes in temperature.

Due to warming and intensified runoff, CO_2 consumption and P release increase in our simulations (Figures 1c and 1d). The spatial changes in chemical weathering vary between the models (Figure 2). Most models show an increase in weathering in midlatitude to high-latitude regions, whereas changes in (sub)tropical regions differ in strength and sign. Increases in weathering are mainly driven by warming as shown by the differences in the linear trends between the STD simulations and the simulations in which temperatures were kept on preindustrial level (Tfix)(Figures 1c and 1d). Globally, the increasing runoff rates during the twentieth century have increased chemical weathering, with the exception of the MIROC-ESM runoff. Regionally, decreases in runoff can lead to reduced weathering rates. However, the reconstructed runoff differs strongly among the ESMs.

The trends in the simulated CO_2 consumption are in line with earlier studies. A 4–14% increase in the chemical weathering rate for each degree of temperature increase was reported for eight Iceland river catchments [*Gislason et al.*, 2009]. Our model simulates a 9% increase in global chemical weathering for each degree

of temperature increase. When applied with the original climatic data of *Gislason et al.* [2009], the model shows a slightly higher-temperature sensitivity of the weathering flux for the Iceland catchments but overall compares well with the river discharge data (supporting information). A 2–28% increase in the chemical weathering rate for each 100 ppmv increase was found in a process-based model depending on the lithology [*Beaulieu et al.*, 2010, 2012]. We found a 13% increase per 100 ppmv, globally. Comparable estimates for P release are not known to the authors. The effect of the runoff biases in the climate reconstructions on the relative increase in weathering rates is negligible, although the absolute numbers are affected, as they depend on the baseline fluxes (not shown). The manipulation of the apparent activation energy in the temperature response function of the weathering model has profound effects on the weathering rates, resulting global fluxes which are ± 45% compared to the standard parametrization (Figures 1g and 1h). The hydrological control of chemical weathering might be underestimated by our model, as we do not account for changes in the residence time and pathway of water in the weathering zone [*Maher*, 2011; *Maher and Chamberlain*, 2011]. Thus, to decrease uncertainty a better understanding of the strengths of the climatic controls on weathering and their interactions must be a prior aim.

This study assumes constant land cover and land use. Changes in agricultural areas and land use practices could have significantly altered chemical weathering fluxes [*Hartmann et al.*, 2013], for example, nitrogen fertilization [*Perrin et al.*, 2008], liming, and water management [*Raymond et al.*, 2008] were identified to influence chemical weathering rates in individual catchments. Therefore, the actual change in chemical weathering since 1850 might differ from the change by climate change alone.

3.3. Implications for the Global C Balance

On average 1.4 ± 0.6 Gt C yr^{-1} was taken up by land during last decade which is generally attributed to changes in biological activity [*Le Quere et al.*, 2013]. On the basis of the high sensitivity of CO_2 consumption found in model simulations of the Mackenzie catchment, *Beaulieu et al.* [2012] concluded that weathering has contributed significantly to historical land C uptake. Using a spatially explicit global model of weathering, we estimated the sensitivity of global weathering to historical climate change to be 55% lower than the sensitivity found by *Beaulieu et al.* [2012] but in line with other studies [*Gislason et al.*, 2009; *Beaulieu et al.*, 2010]. It is therefore very questionable if the Mackenzie catchment is representative for the globe and thus if CO_2 consumption by weathering has played a significant role in historical land C balance.

In addition to CO_2 consumption by chemical weathering, changes in P release link chemical weathering to the land C cycle, as P availability constrains the C storage potential of ecosystems. Ecosystems consist of different forms of organic matter, for example, wood, leaves, or soil organic matter, which have rather constrained C to P ratios. We use these stoichiometric ratios of organic matter to calculate how much C can be stored additionally due to increasing P release (supporting information). Our approach must be seen as a first approximation as the fate of the additionally released P is hard to constrain due to gaps in our knowledge of the P cycle [*Wang et al.*, 2010; *Goll et al.*, 2012]. The approximated C uptake due to changes in P release is comparable in magnitude to the CO_2 consumption by chemical weathering but overall relatively small compared to current land C uptake [*Le Quere et al.*, 2013]. The calculations are based on the assumption that all of P released is incorporated into organic matter, which is likely an overestimation. Thus, the actual effect might be even smaller.

Finally, we performed a back of the envelope calculation of the feedback strength of CO_2 consumption and P release. Again, this is a first approximation of the feedback strength, but it helps to put our findings in context to known feedback mechanisms operating on a centennial time scale [*Arneth et al.*, 2010]. We used the simulated changes in CO_2 consumption and the estimated increase in biological C fixation due changes in P release during the twentieth century (supporting information). According to our rough calculation, the feedback strength for CO_2 consumption and P release are -0.02 ± 0.01 W m^{-2} K^{-1} and -0.02 ± 0.01 W m^{-2} K^{-1}, respectively. Although being one magnitude smaller than the C cycle feedback, the chemical weathering feedbacks are comparable in strength to small second-order feedbacks such as methane, fire, or ozone [*Arneth et al.*, 2010].

References

Anav, A., P. Friedlingstein, M. Kidston, L. Bopp, P. Ciais, P. Cox, C. Jones, M. Jung, R. Myneni, and Z. Zhu (2013), Evaluating the land and ocean components of the global carbon cycle in the Cmip5 Earth System Models, *J. Clim.*, *26*, 6801–6843, doi:10.1175/JCLI-D-12-00417.1.

Arneth, A., et al. (2010), Terrestrial biogeochemical feedbacks in the climate system, *Nat. Geosci.*, *3*(8), 525–532, doi:10.1038/ngeo905.

Acknowledgments

We acknowledge the World Climate Research Programme's Working Group on Coupled Modelling, which is responsible for CMIP, and we thank the climate modeling groups (listed in supporting information) for producing and making available their model output. For CMIP the U.S. Department of Energy's Program for Climate Model Diagnosis and Intercomparison provides coordinating support and led development of software infrastructure in partnership with the Global Organization for Earth System Science Portals. Daniel Goll, Jens Hartmann, and Nils Moosdorf are funded through the DFG Cluster of Excellence CLiSAP (EXC 177/2). We thank the three anonymous reviewers for their constructive and thoughtful comments.

The Editor thanks Yves Godderis and Gabriel Filippelli for their assistance in evaluating this paper.

Beaulieu, E., Y. Goddéris, D. Labat, C. Roelandt, P. Oliva, and B. Guerrero (2010), Impact of atmospheric CO2 levels on continental silicate weathering, *Geochem. Geophys. Geosyst.*, *11*, Q07007, doi:10.1029/2010GC003078.
Beaulieu, E., Y. Goddéris, Y. Donnadieu, D. Labat, and C. Roelandt (2012), High sensitivity of the continental-weathering carbon dioxide sink to future climate change, *Nat. Clim. Change*, *2*(5), 346–349, doi:10.1038/nclimate1419.
Berner, R. A., A. C. Lasaga, and R. M. Garrels (1983), The carbonate-silicate geochemical cycle and its effect on atmospheric carbon dioxide over the past 100 million years, *Am. J. Sci.*, *283*, 641–683.
Brands, S., S. Herrera, J. Fernández, and J. M. Gutiérrez (2013), How well do CMIP5 Earth System Models simulate present climate conditions in Europe and Africa?, *Clim. Dyn.*, *41*, 803–817, doi:10.1007/s00382-013-1742-8.
Dai, A., and K. E. Trenberth (2002), Estimates of freshwater discharge from continents: Latitudinal and seasonal variations, *J. Hydrometeorol.*, *3*, 660–687.
Elser, J. J., M. E. S. Bracken, E. E. Cleland, D. S. Gruner, W. S. Harpole, H. Hillebrand, J. T. Ngai, E. W. Seabloom, J. B. Shurin, and J. E. Smith (2007), Global analysis of nitrogen and phosphorus limitation of primary producers in freshwater, marine and terrestrial ecosystems, *Ecol. Lett.*, *10*(12), 1135–1142, doi:10.1111/j.1461-0248.2007.01113.x.
FAO, IIASA, ISRIC, and JRC (2009), Harmonized World Soil Database (version 1.1), *Tech. Rep.*, Rome, Italy and Laxenburg, Austria.
Fekete, B. M. (2002), High-resolution fields of global runoff combining observed river discharge and simulated water balances, *Global Biogeochem. Cycles*, *16*(3), 1042, doi:10.1029/1999GB001254.
Fernandez-Martinez, M., et al. (2014), Nutrient availability as the key regulator of global forest carbon balance, *Nat. Clim. Change*, doi:10.1038/nclimate2177.
Gislason, S. R., et al. (2009), Direct evidence of the feedback between climate and weathering, *Earth Planet. Sci. Lett.*, *277*(1-2), 213–222, doi:10.1016/j.epsl.2008.10.018.
Goll, D. S., V. Brovkin, B. R. Parida, C. H. Reick, J. Kattge, P. B. Reich, P. M. van Bodegom, and U. Niinemets (2012), Nutrient limitation reduces land carbon uptake in simulations with a model of combined carbon, nitrogen and phosphorus cycling, *Biogeosciences*, *9*(9), 3547–3569, doi:10.5194/bg-9-3547-2012.
Hartmann, J., and N. Moosdorf (2011), Chemical weathering rates of silicate-dominated lithological classes and associated liberation rates of phosphorus on the Japanese Archipelago Implications for global scale analysis, *Chem. Geol.*, *287*(3-4), 125–157, doi:10.1016/j.chemgeo.2010.12.004.
Hartmann, J., and N. Moosdorf (2012), The new global lithological map database GLiM: A representation of rock properties at the Earth surface, *Geochem. Geophys. Geosyst.*, *13*, Q12004, doi:10.1029/2012GC004370.
Hartmann, J., N. Jansen, H. H. Dürr, S. Kempe, and P. Köhler (2009), Global CO2-consumption by chemical weathering: What is the contribution of highly active weathering regions?, *Global Planet. Change*, *69*(4), 185–194.
Hartmann, J., A. J. West, P. Renforth, P. Körner, C. L. De La Roche, D. A. Wolf-Gladrow, H. H. Dürr, and J. Scheffran (2013), Enhanced chemical weathering as a geoengineering strategy to reduce atmospheric carbon dioxide, supply nutrients, and mitigate ocean acidification, *Rev. Geophys.*, *51*, 113–149, doi:10.1002/rog.20004.
Hartmann, J., N. Moosdorf, R. Lauerwald, A. J. West, and M. Hinderer (2014), Global chemical weathering and associated P-release-The role of lithology, temperature and soil properties, *Chem. Geol.*, *363*, 145–163, doi:10.1016/j.chemgeo.2013.10.025.
Hijmans, R. J., S. E. Cameron, J. L. Parra, P. G. Jones, and A. Jarvis (2005), Very high resolution interpolated climate surfaces for global land areas, *Int. J. Climatol.*, *25*(15), 1965–1978, doi:10.1002/joc.1276.
Hoenisch, B., N. G. Hemming, D. Archer, M. Siddall, and J. F. McManus (2009), Atmospheric carbon dioxide concentration across the Mid-Pleistocene transition, *Science*, *324*(5934), 1551–1554, doi:10.1126/science.1171477.
Labat, D., Y. Goddéris, J. L. Probst, and J. L. Guyot (2004), Evidence for global runoff increase related to climate warming, *Adv. Water Res.*, *27*(6), 631–642.
Le Quere, C., et al. (2013), The global carbon budget 1959–2011, *Earth. Syst. Sci. Data*, *5*, 165–185, doi:10.3334/CDIAC/GCP.
Maher, K. (2011), The role of fluid residence time and topographic scales in determining chemical fluxes from landscapes, *Earth Planet. Sci. Lett.*, *312*, 48–58, doi:10.1016/j.epsl.2011.09.040.
Maher, K., and C. Chamberlain (2011), Hydrologic regulation of chemical weathering and the geologic carbon cycle, *Science*, *343*, 1502–1504, doi:10.1126/science.1250770.
Moquet, J.-S., et al. (2011), Chemical weathering and atmospheric/soil CO2 uptake in the Andean and Foreland Amazon basins, *Chem. Geol.*, *287*(1-2), 1–26, doi:10.1016/j.chemgeo.2011.01.005.
Peñuelas, J., et al. (2013), Human-induced nitrogen-phosphorus imbalances alter natural and managed ecosystems across the globe, *Nat. Commun.*, *4*, 2934, doi:10.1038/ncomms3934.
Perrin, A.-S., A. Probst, and J.-L. Probst (2008), Impact of nitrogenous fertilizers on carbonate dissolution in small agricultural catchments: Implications for weathering CO2 uptake at regional and global scales, *Geochim. Cosmochim. Acta*, *72*(13), 3105–3123, doi:10.1016/j.gca.2008.04.011.
Probst, J. L., and Y. Tardy (1987), Long range streamflow and world continental runoff since the beginning of this century, *J. Hydrol.*, *94*, 289–311.
Randall, D. A., et al. (2007), Climate models and their evaluation, in *Climate Change 2007: The Pysical Science Basis. Contribution of Working Group I to the Fourth Assessment Report of the Intergovernmental Panel on Climate Change*, edited by Solomon, S. D. et al., chap. Climate Mo, Cambridge Univ. Press, Cambridge, U. K., and New York.
Raymond, P. A., N.-H. Oh, R. E. Turner, and W. Broussard (2008), Anthropogenically enhanced fluxes of water and carbon from the Mississippi River, *Nature*, *451*(7177), 449–452, doi:10.1038/nature06505.
Taylor, K. E., R. J. Stouffer, and G. A. Meehl (2012), An overview of CMIP5 and the experiment design, *Bull. Am. Meteorol. Soc.*, *93*(4), 485–498, doi:10.1175/BAMS-D-11-00094.1.
van der Velde, M., L. See, L. You, J. Balkovič, S. Fritz, N. Khabarov, M. Obersteiner, and S. Wood (2013), Affordable nutrient solutions for improved food security as evidenced by crop trials, *PloS one*, *8*(4), e60075, doi:10.1371/journal.pone.0060075.
Walker, J. C. G., P. B. Hays, and J. F. Kasting (1981), A negative feedback mechanism for the long-term stabilization of Earth's surface-temperature, *J. Geophys. Res.*, *86*, 9776–9782.
Wang, Y. P., R. M. Law, and B. Pak (2010), A global model of carbon, nitrogen and phosphorus cycles for the terrestrial biosphere, *Biogeosciences*, *7*, 2261–2282, doi:10.5194/bg-7-2261-2010.
White, A. F., A. E. Blum, T. D. Bulle, D. V. Vivit, M. Schulz, and J. Fritzpatrick (1999), The effect of temperature on experimental and natural chemical weathering rates of granitoid rocks, *Geochim. Cosmochim. Acta*, *63*(19), 3277–3291.